2013

Interaction Mechanism of Benzene and Phenanthrene in Condensed Organic Matter: Importance of Adsorption (Nanopore-Filling)

Ke Sun

Yong Ran

Yu Yang

Baoshan Xing

Jingdong Mao
Old Dominion University

Original Publication Citation

Sun, K., Ran, Y., Yang, Y., Xing, B. S., & Mao, J. D. (2013). Interaction mechanism of benzene and phenanthrene in condensed organic matter: Importance of adsorption (nanopore-filling). *Geoderma, 204*, 68-74. doi:10.1016/j.geoderma.2013.04.008

Geoderma 204–205 (2013) 68–74

Contents lists available at SciVerse ScienceDirect

Geoderma

journal homepage: www.elsevier.com/locate/geoderma

Interaction mechanism of benzene and phenanthrene in condensed organic matter: Importance of adsorption (nanopore-filling)

Ke Sun [a,1], Yong Ran [a,*], Yu Yang [a], Baoshan Xing [b], Jingdong Mao [c]

[a] State Key Laboratory of Organic Geochemistry, Guangzhou Institute of Geochemistry, Chinese Academy of Sciences, Guangzhou 510640, China
[b] Stockbridge School of Agriculture, University of Massachusetts, Amherst, MA 01003, USA
[c] Department of Chemistry and Biochemistry, Old Dominion University, Norfolk, VA 23529, USA

ARTICLE INFO

Article history:
Received 8 November 2012
Received in revised form 11 April 2013
Accepted 12 April 2013
Available online 14 May 2013

Keywords:
Sorption and desorption
Condensed NOM
Benzene
Phenanthrene
Microporosity

ABSTRACT

Although microporosity and surface area of natural organic matter (NOM) are crucial to mechanistic evaluation of the sorption process for nonpolar organic contaminants (NOCs), they have wrongly been estimated by the N_2 adsorption technique. Nuclear magnetic resonance spectroscopy (^{13}C NMR), and benzene, carbon dioxide, and nitrogen adsorption techniques were used to characterize structural and surface properties for different condensed NOM samples, which were related to the sorption behavior of phenanthrene (Phen). It was found that the revised Freundlich model by taking the chemical activity into account can well describe the isotherms for benzene and Phen. The benzene and Phen adsorption volumes for the coal samples are similar to or lower than the CO_2-nanopore volumes. Adsorption volumes of both benzene and Phen are significantly related to the aliphatic carbon structure, and their correlation lines are nearly overlapped, suggesting that the nanopore filling for Phen and benzene on the investigated samples is the dominating mechanism, and also is not affected by water molecules. The entrapment of benzene and/or the pore deformation in the NOM nanopore are likely responsible for the observed hysteresis of benzene. The above results demonstrate that Phen and benzene adsorption on the condensed NOM is closely associated with the aliphatic carbon structure of the investigated samples.

1. Introduction

Sorption and sequestration of nonpolar organic chemicals (NOCs) by natural organic matter (NOM) associated with aquifers, soils, sediments (geosorbents) control bioavailability, risk, and biodegradation of NOCs (Brusseau et al., 1991; Chefetz and Xing, 2009; Pignatello and Xing, 1996). Many investigations during the last three decades identified that the organic matter types and microporosity are important for the sorption of NOCs (Chefetz and Xing, 2009; Chen and Xing, 2005; Grathwohl, 1990; Plaza et al., 2009; Salloum et al., 2002; Senesi, 1992). However, the physicochemical mechanisms of sorption/desorption and reduced bioavailability are limited.

The chemical and structural properties of NOM strongly affect the sorption and desorption of NOCs in soils and sediments (Chefetz and Xing, 2009; Pignatello and Xing, 1996; Weber et al., 1992). Previous investigations indicated that various types of bulk SOM with high aliphatic carbon showed strong sorption for phenanthrene and pyrene (Chefetz et al., 2000; Mao et al., 2002). NOM has been characterized as comprising dual domains or components that exhibit distinctly different sorption reactivity (Grathwohl, 1990; Kleineidam et al., 2002; Ran et al., 2004; Weber et al., 1992; Xing and Pignatello, 1997). Depending on parental sources and diagenetic alteration histories, NOM may comprise different types of organic materials ranging from biopolymer, humus, kerogen and coal materials, and black carbon. Condensed organic carbons such as kerogen, coal, and black carbon can substantially contribute to NOM in soils and sediments (Cornelissen et al., 2005; Ran et al., 2002, 2007; Weber et al., 1992). It is noted that NMR spectroscopy has been increasingly used to provide a basis for inferring the molecular structure in these organic matter (Chefetz et al., 2000; Filimonova et al., 2004; Kögel-Knabner, 1997; Ran et al., 2002, 2007; Salloum et al., 2002).

Surface and geometric heterogeneity in NOM could be very important for the sorption mechanism of NOCs on NOM. The surface area of NOM is crucial to the mechanistic interpretation of sorption process. N_2 adsorption was recommended as the standard method to measure the surface area of soils/sediments (Gregg and Sing, 1982). However, large discrepancies were reported between NOM surface areas derived from CO_2 adsorption and N_2 adsorption, primarily because of the activated diffusion phenomenon (Aochi and Farmer, 2005; de Jonge and Mittelmeijer-Hazeleger, 1996; Li and Werth, 2001; Ran et al., 2013; Ravikovitch et al., 2005; Xing and Pignatello, 1997). Carbon dioxide at 273 K and benzene at 295 K have been used as alternative gases for probing the surface properties of carbonaceous materials (Corley et al., 1996;

* Corresponding author. Tel.: +86 20 85290263; fax: +86 20 85290706.
E-mail address: yran@gig.ac.cn (Y. Ran).
[1] Present address: State Key Laboratory of Water Environment Simulation, School of Environment, Beijing Normal University, Beijing 100875, China.

0016-7061/$ – see front matter © 2013 Elsevier B.V. All rights reserved.
http://dx.doi.org/10.1016/j.geoderma.2013.04.008

de Jonge and Mittelmeijer-Hazeleger, 1996; Gan et al., 1972; Kwon and Pignatello, 2005; Larsen et al., 1995; Ravikovitch et al., 2005; Reucroft and Sethuraman, 1987; Walker and Kini, 1965; Xing and Pignatello, 1997). Glassy forms of NOM including humin, kerogen and coals have internal microporosity that apparently is not accessed by N_2 at 77 K due to activation diffusion. Moreover, previous investigations demonstrated that the adsorption (hole-filling) mechanism is important for the sorption of hydrophobic organic contaminants by the isolated kerogen, Pahokee peat, and coals (Ran et al., 2002, 2004, 2013). However, how the microporosity measured by CO_2 and benzene gas molecules is related to the structure of NOMs and the aqueous sorption capacity for NOCs on various NOMs has not yet been systematically investigated.

This study investigates how the hydrophobic nanopore volumes measured with benzene vapor and CO_2 gas are related to the structure of NOM and the sorption capacity of phenanthrene (Phen) on a range of condensed NOM samples, and how the adsorption of aqueous Phen is related to that of gaseous benzene, and is affected by water molecules. We hypothesized that the hydrophobic nanopore in glassy NOM could be large enough for accommodating majority of NOCs. We used a wide range of condensed NOM ranging from nonhydrolyzable organic carbon (NHC) to black carbon (BC) and coals (Table 1) as sorbents, and Phen and benzene vapor as model sorbates to test this hypothesis.

2. Materials and methods

2.1. Sorbents and characterization

Two surface soil samples (HP04 and HP05) were collected to a depth of 20 cm in July 2002 from Hangpu district of Guangzhou city, China. Three surface sediment samples (C01, C03, and C08) (0–20 cm) were collected from the Pearl River Estuary (PRE) using a box sampler in August 2002. The water depth was 25 m for C01, 25 m for C03, and 69 m for C08. The soils and sediments were treated using an acid hydrolysis method and a combustion method at 375 °C for the separation of five nonhydrolyzable carbon (NHC) and one black carbon (BC) samples, respectively (Ran et al., 2007). Specifically, carbonates were first dissolved in 1 N HCl for 24 h. The residual fractions were treated with 1 N HCl and 10% HF for 5 days, which was repeated four times. Polysaccharides were released by trifluoroacetic acid (TFA) hydrolysis. Finally, the residual hydrolyzable organic matter was removed with 6 N HCl at 110 °C for 24 h. The residues (NHC) were obtained. An aliquot of NHC was heated at 375 °C for 24 h with sufficient air for the BC isolation. It is noted that that determining BC by heating at 375 °C is an accepted but somewhat arbitrary procedure. Many components of BC substrates vanish at lower temperatures, while at least portions of mineral-associated humic substances (not BC) resist to that temperature. In addition, Beulah-Zap lignite (BZ) was obtained from the American Argonne Premium coals. A lignite coal (JP), two bituminous coals (XW and XA), and an anthracite (YX), were collected from state-owned coal mines and covered a wide range of maturity with vitrinite reflectance (R_o) from 0.52% to 2.50% (Chen et al., 2005).

The C, H, O, and N contents were measured using an Elementar Vario ELIII or a Heraeus CHN-O-RAPID elemental analyzer. Specific surface areas (SSA) and microporosity were measured using the N_2-adsorption and CO_2-sorption techniques, at the normal boiling temperature (77 K) and at 273 K in a Micromeritics ASAP 2010 instrument and Autosorb-1 gas analyzer (Quantachrome Instrument Corp., Boynton Beach, FL), respectively (Ran et al., 2013). The ^{13}C CP/TOSS (cross polarization/total sideband suppression) NMR spectra for the five coals were obtained on a Bruker Avance-400 NMR spectrometer operated at a ^{13}C frequency of 100 MHz and at a magic-angle-spinning (MAS) rate of 6.0 kHz. Briefly, the solid coal samples were placed in a 4-mm diameter ZrO_2 rotor with a Kel-F cap. A 1.2-s recycle delay and a 1-ms contact time were used. Between 3500 and 4500 scans were collected. The physicochemical properties of the investigated samples are summarized in Table 1.

2.2. Sorption and desorption experiments

Adsorption isotherms of benzene vapor were recorded at 23 °C with an intelligent gravimetric analyzer (IGA supplied by Hidden Analytical Ltd). Benzene isotherms were obtained by setting pressure intervals relative to saturation vapor pressure (p/p_o) at 298 K. Prior to the measurements, the adsorbent was outgassed in situ until constant weight was achieved at a temperature of 373 K. About 70 mg of a given sample was loaded for each run. HPLC grade benzene was used as adsorbate. Pressure steps in the range of p/p_o values 0–0.94 were used to obtain the isotherm. The equilibrium time for each point of the sorption isotherms ranged from tens of minutes to several hours.

The completely mixed batch reactor (CMBR) systems were employed for the Phen sorption isotherms at room temperature (23 °C). The equilibrium time is four weeks. Flame-sealed glass ampules (50 ml) were used as the CMBRs. The experiments consisted of preliminary tests and final equilibrium tests. The average concentrations of Phen detected in the control reactors were within 98–102% of the initial concentrations. No correction for solute loss was made during the reduction of sorption data. Solute concentrations of the initial aqueous solutions and equilibrated aqueous solutions were analyzed on a reversed-phase HPLC (Hewlett-Packard model 1100, ODS, 5 μm, 2.1 × 250 mm C-18 column) with both diode array UV

Table 1
Physicochemical properties for the samples[a,b].

Samples	C %	H %	N %	O %	O/C	H/C	N_2-SSA m^2/g	N_2-V_o μl/g	CO_2-SSA m^2/g	CO_2-V_o μl/g	Ash %	R_o %
C01	36.9	2.49	0.38	9.26	0.19	0.81	13.3	nd[c]	nd	nd	50.97	nd
C03	23.2	1.82	0.23	7.49	0.24	0.94	7.93	nd	nd	nd	67.26	nd
C08	34.4	2.71	0.46	8.80	0.19	0.94	15.8	nd	nd	nd	53.63	nd
HP04	50.7	2.45	0.32	13.6	0.20	0.58	4.28	nd	nd	nd	32.93	nd
HP05	52.3	3.72	0.56	16.7	0.24	0.85	6.71	17	133	55.0	26.72	nd
HP05BC	17.3	0.77	0.18	3.09	0.13	0.12	16.7	nd	nd	nd	78.66	nd
BZ	68.1	4.51	1.07	19.0	0.21	0.79	1.74	6.0	206	85.0	6.59	0.50
JP	68.6	4.35	3.85	14.9	0.16	0.76	4.91	10	169	73.0	8.10	0.52
XA	73.2	3.62	4.14	3.63	0.04	0.59	1.61	6.0	146	48.7	13.91	1.70
XW	48.7	3.17	3.19	6.34	0.10	0.78	6.92	19	85.0	26.3	38.10	1.12
YX	82.5	3.22	0.53	1.75	0.02	0.47	2.57	10	253	84.0	8.93	2.50

[a] R_o, vitrinite reflectance; N_2-SSA, N_2-derived specific surface area; CO_2-SSA, CO_2-derived specific surface area; N_2-Vo, N_2-derived micropore volume; CO_2-V_o, CO_2-derived internal hydrophobic microporosity.

[b] The elemental compositions and reflectance (R_o %) were cited for the JP, XA, XW, and YX coals from Chen et al. (2005), for the BZ lignite from Larsen et al. (1995), and for the NHC (C01, C03, C08, HP04, and HP05) and BC (HP05BC) samples from Ran et al. (2007).

[c] nd, not determined.

and fluorescence detector as described previously (Ran et al., 2002). The solid-phase solute concentrations were computed based on the mass balance of the solute between the two phases.

2.3. Sorption and desorption modeling

The sorption equilibrium isotherms were fitted using SYSTAT software (Version 8.0, SYSTAT Inc.) to the revised Freundlich model

$$\log\ q_e = \log\ K_F + n\ \log\ C_r \quad (1)$$

where q_e is the equilibrium solid-phase solute concentration; K_F and n are the Freundlich capacity parameter and the isotherm nonlinearity factor, respectively; C_r is the dimensionless aqueous phase concentration or gas phase pressure (p/p_o). For weakly polar and sparsely soluble compounds, C_r is related to solute activity (a) in water phase referenced to their respective pure liquid or supercooled liquid (scl) state at a given temperature (Carmo et al., 2000). For NOCs that are solid at the experimental temperature condition, C_r is the ratio of C_e to S_{scl}. S_{scl} for Phen is 5.18 mg/l (Ran et al., 2002). The sorption capacity parameter K_F can be normalized with OC (K_{FOC}) (Ran et al., 2004).

3. Results and discussion

3.1. Characterization of the condensed NOM

The C contents, O/C ratios, H/C ratios of the samples range from 17.3% to 82.5%, from 0.02 to 0.24, and from 0.12 to 0.94, respectively (Table 1). The O/C and H/C atomic ratios for the NHC fractions, when plotted on the Van Krevelen diagram (Fig. 1), are similar to those of the coals (kerogen type III) derived mainly from higher plant materials, which is rich in lignin with aromatic structure. The coal samples cover a wide range of NOM maturity as vitrinite reflectance (R_o) varies between 0.50% and 2.50%. As dia- and catagenesis for the NOM fractions are developed, the atomic O/C and H/C ratios decrease, but the maturity index (R_o) increases. The O/C ratios for NHC are much lower than the average O/C ratios (0.53) for typical humic acids (HAs) extracted from soils and sediments (Ran et al., 2007; Xing and Pignatello, 1997). The BC sample (HP05BC) combusted at 375 °C from the soil sample has the lowest H/C ratio and quite low O/C, suggesting that BC has the highest degree of maturation among the investigated samples.

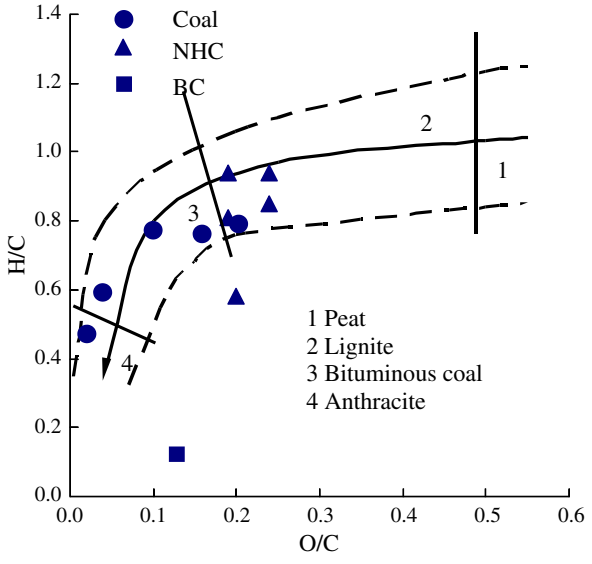

Fig. 1. The van Krevelen diagram for the NHC (C01, C03, C08, HP04, and HP05, solid triangle), different ranks of coals (BZ, JP, XA, XW, and YX, solid circle) and BC (HP05BC, solid square) samples in Table 1. The arrow line represents the evolution pathway of chemical composition as diagenetic alteration continues for the kerogen type III. The numbers (1, 2, 3, and 4) represent different maturation stages for the investigated NOM.

The measured SSA based on N_2 adsorption at 77 K (N_2-SSA) for the NHC, BC, and coals ranges from 1.61 to 16.69 m^2/g (Table 1). However, the surface areas of the coals based on CO_2 adsorption at 273 K (CO_2-SSA) are much higher (85–253 m^2/g) (Table 1), which are in the same order of magnitude as coals (118–207 m^2/g) reported by Vorres (1990). Moreover, previous investigation showed that N_2-SSA increased as the ash content increased and organic carbon (OC) content decreased, but CO_2-SSA was positively related to OC contents and inversely correlated with the ash contents (Ran et al., 2013). Hence, N_2 and CO_2 probe different regions of the NOM matrices. N_2 is adsorbed primarily on the external surface of NOM and mineral particles, while CO_2 additionally probes the internal porosity of NOM.

The ^{13}C NMR spectra of the coals are presented in Fig. 2 and those of NHC are cited from our previous publication (Ran et al., 2007). The integration results are shown in Table S1 in the Supplemental data. Approximate band assignments are as follows: nonpolar alkyls (0–45 ppm), methoxy (45–63 ppm), O-alkyls (63–93 ppm), aromatics (93–148 ppm), aromatic C–O (148–165 ppm), carboxylic carbon (165–187 ppm), and ketones, quinones, and aldehydes (187–220 ppm). The spectra of YX and XA are dominated by aromatic signals at around 130 ppm, and only very small aliphatic signals at 0–50 ppm are present. The spectrum of XW is also dominated by aromatic signals but its aliphatic signals are more intense than those of YX or XA. Both of the aromatic (93–165 ppm) and aliphatic signals (0–93 ppm) for the spectra of JP and BZ are significant (Fig. 2). As thermal maturity of the samples increases, their aromaticity increases while their aliphaticity is reduced. For the investigated coals, the aromaticity increases from the lignite (JP and BZ) to the bituminous coal (XW and XA), and to the anthracite coal (YX) (Table S1). For the NHC samples, the aromaticity is close to

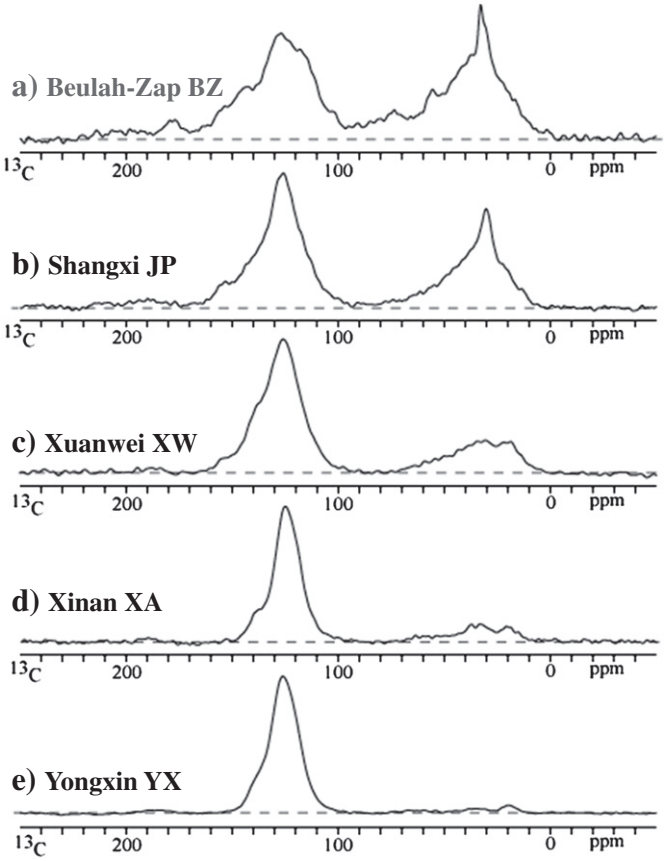

Fig. 2. Cross-polarization/magic angle spinning (CP/MAS) ^{13}C nuclear magnetic resonance (NMR) spectra for the investigated coals.

that of the lignite except for the HP04 sample. HP04 is similar to the bituminous coal XW (Table S1). The above result is consistent with that demonstrated from the Van Krevelen diagram (Fig. 1).

3.2. Sorption and/or desorption isotherms

The sorption isotherms for Phen by the investigated samples are shown in Fig. S1 in the Supplemental data and their revised Freundlich modeling parameters are listed in Table 2. It is clear from Table 2 that the revised Freundlich equation describes the sorption isotherms for Phen quite well in the entire C_e ranges. The revised Freundlich sorption capacity K_{FOC} ranges from 49.0 μl/g OC to 113 μl/g OC for the NHC and BC isolated from the investigated soils and sediments, and from 24.1 μl/g OC to 79.0 μl/g OC for the coals (Table 2). The nonlinearity factor n for Phen ranges from 0.48 to 0.85.

The sorption/desorption isotherms for the benzene vapors are shown in Fig. S1. The isotherms are nonlinear and exhibit obvious hysteresis. The Freundlich sorption/desorption parameters for benzene at relative pressure from $p/p_o = 0$ to $p/p_o = 0.3$ are summarized in Table 3. At lower relative pressure ($p/p_o < 0.3$), the benzene sorption isotherms are well fitted to the nonlinear Freundlich model for the investigated samples. The isotherms for benzene are strongly nonlinear, with n ranging from 0.221 to 0.598 for the sorption and 0.097 to 0.349 for the desorption (Table 3).

It is obvious that the benzene isotherms are more nonlinear than the Phen isotherms, which may be related to the fact that the benzene vapor adsorption on the minerals does not compete with the water molecule adsorption. In water solutions, the adsorption of NOCs by soil minerals is suppressed by water, and the soil uptake consists primarily of solute sorption into the organic matter (Chiou et al., 1988). Moreover, previous investigations reported the different adsorption behaviors for benzene vapor on soils and sediments. Chiou and Shoup (1985) reported that vapor sorption isotherms of benzene and other organic liquids on soil humic acid were highly linear over a wide range of p/p_o, which was attributed to the partitioning of organic compounds in soil humic acid. However, Lin et al. (1996) found that sorption equilibrium of benzene by a dry soil was well described by the nonlinear Freundlich isotherm ($n < 0.42$). As the relative humidity increased from zero to 33%, the isotherm gradually changed from nonlinearity to linearity, and the soil sorption capacity decreased. Farrell and Reihard (1994a,b) suggested that the existence of intragrain microporosity on micro- and mesoporous silica gels or glass beads may be responsible for the nonlinearity of gaseous NOC isotherm. For the samples in this investigation, the NOM contents and nanopore volumes derived from the CO_2 adsorption are quite high and the ash contents are quite low, especially for coals and HP05 (Table 1). Hence, the minerals in the investigated samples are not responsible for the observed nonlinear sorption isotherms.

Table 2
Revised Freundlich sorption parameters for Phen.

Samples	$K_{F(\mu l/g)}$	$K_{FOC(\mu l/g\ OC)}$[a]	SE[b]	n	SE[c]	R^2	N[d]
C01	31.1	84.2	0.347	0.67	0.028	0.99	24
C03	26.0	112	0.169	0.68	0.018	0.99	24
C08	44.4	129	0.534	0.70	0.024	0.99	24
HP04	21.6	42.6	0.155	0.62	0.011	0.99	24
HP05	39.3	75.1	0.280	0.70	0.015	0.99	23
HP05BC	20.5	118	0.297	0.48	0.020	0.99	20
BZ	71.4	73.0	0.557	0.70	0.020	0.98	22
JP	50.0	44.7	0.431	0.73	0.032	0.99	22
XA	32.7	31.4	0.456	0.85	0.047	0.98	19
XW	15.3	21.8	0.130	0.66	0.027	0.99	22
YX	19.9	24.1	0.314	0.68	0.044	0.97	20

[a] OC normalized Freundlich K_F.
[b] Standard error of K_F.
[c] Standard error of n.
[d] Number of observations.

The sorption capacity parameters (K_F) for Phen and benzene are in the ranges of 18.7–53.8 μl/g and 18.2–79.4 μl/g, respectively (Tables 2 and 3). Apparently, the K_F value for benzene is similar to that of Phen on each of the investigated samples. Moreover, the K_F value for benzene or Phen on each of the four coals (except YX) and HP05 is similar to or slightly lower than the nanopore volume based on the CO_2 adsorption (Tables 1–3). In addition, the correlation analysis indicated that the K_{FOC} values of benenze and Phen are highly correlated ($R^2 = 0.685$) (Fig. S2 in the Supporting data). As this correlation can only account for 68.5% of the variability, other sorbent properties such as pore size and pore surface chemistry may account for the remaining variability. However, the adsorption volume of Phen or benzene is much lower than that of CO_2 on the YX anthracite, which is possibly related to its nanopore size. This above fact indicates that benzene or Phen is able to fill in the similar nanopores of NOM. The above modeling demonstrates that the nanopore filling mechanism is the dominating sorption mechanism for the investigated gaseous benzene molecules and aqueous Phen molecules.

The nonlinear sorption of NOCs has often been attributed to the chemical heterogeneity of NOM using dual-mode sorption model. However, surface and structural heterogeneity could also lead to the nonlinear sorption isotherms, which is well demonstrated in the adsorption of gas molecules and NOCs by activated carbons. The surface and structural heterogeneity including pore size and shape, pore volume, and pore surface chemistry is critical to the adsorption of NOCs on the activated carbon materials. Dubinin (1960) and Crittenden et al. (1999) reported that the adsorption capacity V_o and the exponent term b for the Polanyi–Dubinin model (PDM) were only related to the nature of the adsorbent. For an activated carbon and a synthetic glassy polymer, V_o values were close to or approximately half the experimental total pore volumes, respectively. The b values for adsorption of tens of organic chemicals on the activated carbons (1.1–1.3) were generally lower than on the synthetic glassy polymers (1.4–1.7) (Crittenden et al., 1999). We compared the revised Freundlich model with that of the Polanyi–Dubinin–Manes model, and found that the exponent term b was close to 1. Hence, we only used the Freundlich model to explain our experimental data. When $b = 1$, the revised Freundlich model is a special form of PDM model.

3.3. Sorption and desorption hysteresis of benzene vapor

The desorption hysteresis indices (HI) ($n_{desorption}/n_{sorption}$) for benzene are presented in Table 3. As HI is smaller, the desorption hysteresis is larger. It is observed that different degrees of desorption hysteresis are present for the NHC and coal samples. The most likely explanation for the hysteresis of benzene in these samples is the irreversible pore deformation and entrapment of sorbing molecules (Weber et al., 2002). As benzene enters the solid, it could be adsorbed in nanopores in the open sectors. Hydrophobic sorbate molecules may also expand or penetrate condensed NOM matrices at high q_e, generating "tenant pores" in which they then reside (Braida et al., 2001; Huang and Weber, 1997). This matrix expansion process is highly dependent on the compatibility (similarity of solubility parameters) of the sorbate and the NOM matrices and is likely rate-controlled by diffusion process (Huang and Weber, 1997; Pignatello and Xing, 1996). In the desorption stage, the aqueous-phase solute concentration decreases abruptly, and the NOM configuration may be changed. In addition, Fig. 3 shows that the HI values are inversely related to the OC contents and are positively correlated with the ash contents ($p < 0.01$), suggesting that the organic matter is the major factor for the hysteresis of benzene. This pore deformation mechanism could in part explain the observed desorption hysteresis of benzene at high benzene pressure ($p/p_o > 0.3$).

Entrapment of benzene in the nanopore is also important for the investigated samples. XA and YX are high-rank coals with R_o of 1.7% and 2.5%, respectively (Table 1). It is noted that their glassy-transition temperatures are higher than 600 K (Pignatello and Xing, 1996). Hence,

Table 3
Revised Freundlich sorption and desorption parameters and desorption hysteresis indices for benzene on the samples.

Samples	Sorption						Desorption						Hysteresis Index(HI)
	$K_{F(\mu l/g)}$	SE^a	$n_{sorption}$	SE^b	R^2	N^c	$K_{F,(\mu l/g)}$	SE	$n_{desorption}$	SE	R^2	N	$n_{desorption}/n_{sorption}$
C01	43.4	0.95	0.60	0.017	1.00	9	39.1	0.24	0.23	0.006	0.99	9	0.334
C03	20.5	0.39	0.47	0.014	1.00	9	25.1	0.66	0.31	0.010	0.99	9	0.559
C08	42.4	2.16	0.49	0.011	1.00	9	52.6	2.00	0.35	0.016	0.99	9	0.635
HP04	23.7	0.64	0.59	0.026	0.99	9	24.4	0.59	0.21	0.009	0.99	9	0.306
HP05	47.4	1.75	0.47	0.026	0.99	9	27.9	0.80	0.31	0.011	0.99	9	0.507
HP05BC	12.8	0.16	0.22	0.010	0.99	9	13.9	0.23	0.13	0.006	0.99	9	0.588
JP	79.4	1.49	0.53	0.012	1.00	9	106.3	1.68	0.19	0.006	0.99	9	0.36
XA	15.6	0.70	0.48	0.029	0.99	9	19.9	0.35	0.15	0.006	0.99	9	0.29
XW	23.2	0.50	0.42	0.007	1.00	9	25.0	1.02	0.25	0.015	0.97	9	0.496
YX	35.8	0.93	0.45	0.026	0.99	9	38.2	0.41	0.10	0.003	0.99	9	0.198

[a] Standard error of K_F.
[b] Standard error of n.
[c] Number of observations.

their NOM structures are the most rigid, and should be the least expanded by benzene among the investigated samples. However, they showed the highest hysteresis (Table 3). For HP05BC, it also shows the higher NOM maturation degree (Fig. 1), and the higher rigid NOM structure, although its O/C atomic ratio is slightly higher than that of XA or YX. However, it also exhibits one of the lowest hysteresis among the samples (Table 3). The above phenomenon may be related to the NOM structure and nanopore size distribution. Transmission electron microscopy illustrated that pore diameters in exinite and inertinite of coals ranged from 20 to 100 nm, with most of the pores varying from 2 to 50 nm, but those in vitrinite were smaller than 2 nm (Harris and Yust, 1976). In kerogen samples at low and medium

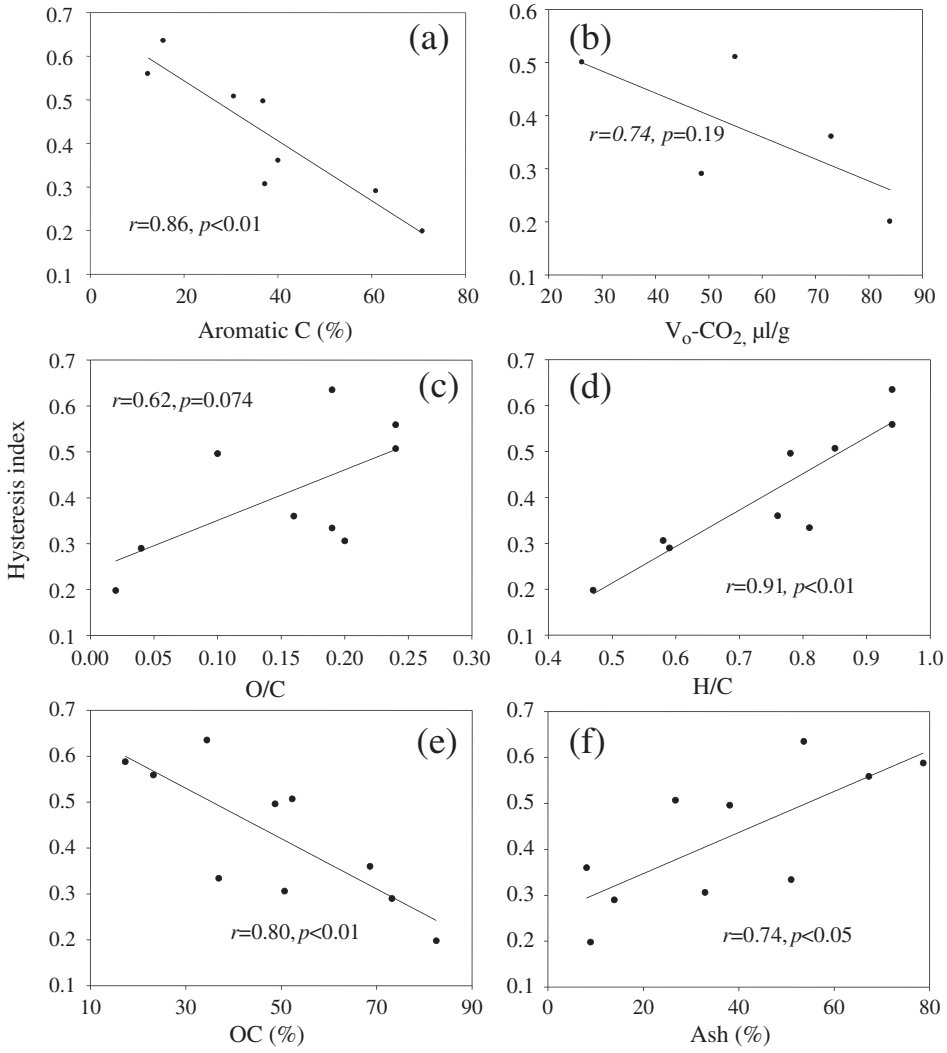

Fig. 3. Correlations between hysteresis index of benzene and the aromatic C (a), volume obtained from CO_2 adsorption isotherm (a), ratios of O/C (c) and H/C (d), organic carbon (OC) (e), and ash contents (%) (f) on the investigated samples.

degrees of catagenesis, the interlayer spacings are widely spread (0.34–more than 0.8 nm), probably due to the fixation of non-aromatic groups on the graphitic layer which prevent them from getting closer. As catagenesis progresses, the non-aromatic groups begin to disappear and the interlayer spacing spreading decreases (Durand, 1980). Moreover, the correlation analysis shows that the HI values are significantly related to the aromaticity and H/C, and marginally significantly to nanopore volume and O/C and H/C ratios for the samples (Fig. 3). As the aromaticity is elevated, and O/C and H/C ratios are reduced, the NOM maturation is elevated, and the benzene hysteresis increases. As the nanopore volume derived from the CO_2 sorption is the higher, the more benzene is trapped in the NOM matrix. In addition, previous investigation demonstrated that aromatic NOCs can form the specific π–π bonds with the aromatic rings of the condensed NOM (Zhu et al., 2004). Huang and Weber (1997) also observed that the desorption hysteresis of Phen was closely associated with the aromatic C of the peat, shale, and kerogen samples. The above result suggests that the entrapment of benzene in NOM nanopore and aromatic graphitic interlayers is likely responsible for the observed hysteresis of benzene.

3.4. Relationship of adsorption with sorbent properties

The K_{FOC} values for Phen and benzene are related to some of the physicochemical properties for the condensed NOM (Fig. 4). They are significantly related to the aliphatic carbons ($p < 0.01$) and inversely correlated with the aromatic carbons of the NOM ($p < 0.01$). Moreover, the positive correlations between K_{FOC} and H/C or O/C ratios for Phen on the investigated samples are significant (Fig. 4). The observed significant correlations are generally consistent with prior studies except for that between K_{FOC} and O/C ratios (Chen and Xing, 2005; Ran et al., 2007). In this investigation, as the O/C ratio is significantly related to H/C ratio ($R^2 = 0.55$) for the investigated samples, the O/C ratio is naturally related to K_{FOC}. Furthermore, previous investigations indicated that various types of bulk SOM with high aliphatic carbon exhibited strong sorption to phenanthrene and pyrene (Chefetz et al., 2000; Salloum et al., 2002). The prior study also demonstrated that the aliphatic groups of the NHC samples played a dominant role in the sorption of Phen (Ran et al., 2007). This investigation suggested that even the coal samples with different NOM maturation degrees also showed the similar phenomenon. In addition, the nearly overlapped correlations between K_{FOC} and aliphatic carbon for Phen and benzene (Fig. 4) suggest that water molecules could not affect the nanopore filling of NOM on the condensed NOM. Hence, the above results further suggest that the NOM structures and nanopores are responsible for the observed difference in the adsorption capacity for the gaseous benzene and the aqueous Phen.

As the NHC fractions and the low maturation coals contain high polymethylene carbon, they exhibit high sorption capacity for benzene and Phen. The glassy and resistant aliphatic carbon might be more nonpolar than the corresponding aromatic carbon with oxygen-containing functional groups. Moreover, as the OM maturation for YX is the highest, the spacings between aromatic interlayers are the smallest. The Phen and benzene molecules could not enter a portion of the aromatic interlayers, but the CO_2 molecules could enter all of the aromatic interlayers. Hence, the Phen or benzene adsorption volume is much lower than the CO_2 adsorption volume on the YX anthracite (Tables 1–3). This study further suggests that the NOM nanopore size has an important influence on the NOC adsorption.

Two possible types of adsorption sites had been proposed for carbonaceous geosorbents (Cornelissen et al., 2005): (i) adsorption on the external surface, and (ii) adsorption in nanopores inside the sorbents. In this study, the N_2-SSA of the condensed NOM is a measure of the outer surface on the minerals and organic matter. But, the CO_2-SSA of coals were found to be one to two orders of magnitude higher than the N_2-SSA, and the adsorption volume CO_2-V_o is close to the benzene and Phen adsorption volume estimated by the revised Freundlich model. These results further provide the direct evidence to support our hypothesis that the adsorption in nanopores is the dominant mechanism for the sorption of Phen and benzene on the condensed NOM. Furthermore, this study shows that the condensed NOMs rich in aliphatic carbons have higher adsorption volumes for benzene and Phen.

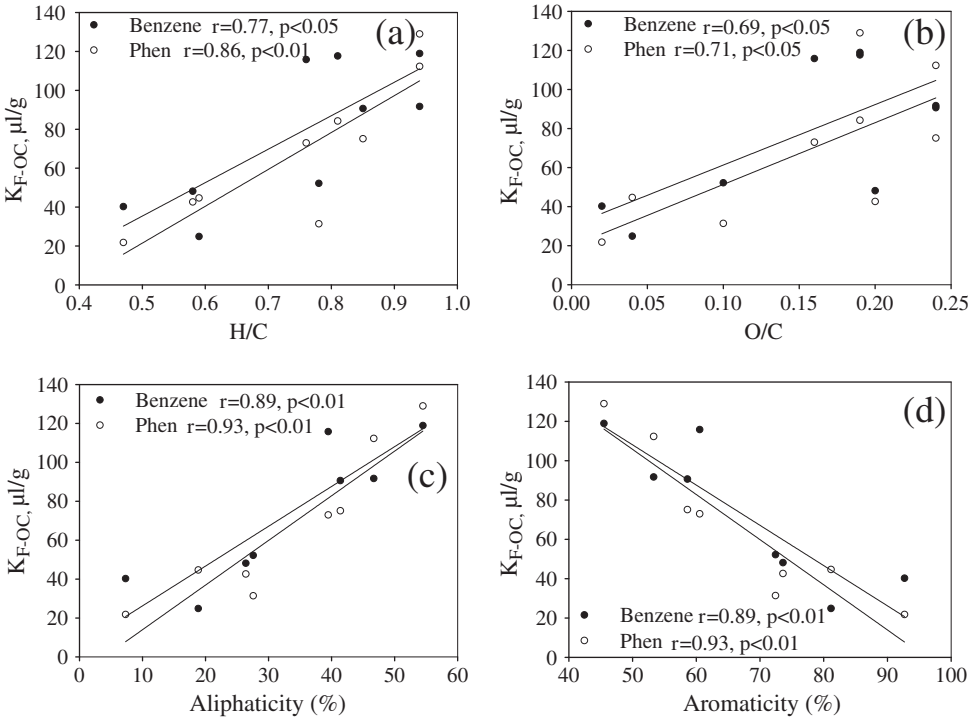

Fig. 4. Correlation of the phenanthren (Phen) and benzene capacity parameters with physicochemical properties of the samples. Aliphaticity% = 100 − Aromaticity%, which is listed in Table S1 in the Supplemental data.

4. Conclusions

The above results provide important implications for the interpretation of sorption mechanisms of organic contaminants in SOM. Our data support the concept of "adsorption" of NOCs in the internal nanopores of NOM. Moreover, quantitative estimates of nanopore and surface area derived from the CO_2 or benzene adsorption allow for a more specific formulation of this concept. The majority of total surface area is formed by nanometer scale pores. Finally, the findings suggest a possible mechanism for sequestration of chemicals.

Acknowledgments

This study was supported by a key project of NNSFC-Guangdong (U1201235), a general project and a "Team Project" of National Natural Science Foundation of China (41073082 and 41121063), and GIGCAS 135 project (Y234081001). JDM thanks the National Science Foundation (CBET-0853950). This is contribution No. IS-1630 from GIGCAS.

Appendix A. Supplementary data

One table containing the integral results of ^{13}C NMR spectra, one figure illustrating the sorption and desorption isotherms of benzene and Phen sorption isotherms, and one figure showing the correlation between the adsorption volumes of benzene and Phen. Supplementary data to this article can be found online at http://dx.doi.org/10.1016/j.geoderma.2013.04.008.

References

Aochi, Y.O., Farmer, W.J., 2005. Impact of soil microstructure on the molecular transport dynamics of 1,2-dichloroethane. Geoderma 127, 137–153.
Braida, W.J., White, J.C., Ferrandino, F.J., Pignatello, J.J., 2001. Effect of solute concentration on sorption of polyaromatic hydrocarbons in soil: uptake rates. Environmental Science and Technology 35, 2765–2772.
Brusseau, M.L., Jessup, R.E., Rao, P.S.C., 1991. Nonequilibrium sorption of organic chemicals: elucidation of rate-limiting processes. Environmental Science and Technology 25, 134–142.
Carmo, A.M., Hundal, L.S., Thompson, M.L., 2000. Sorption of hydrophobic organic compounds by soil materials: application of unit equivalent Freundlich coefficients. Environmental Science and Technology 34, 4363–4369.
Chefetz, B., Xing, B., 2009. Relative role of aliphatic and aromatic moieties as sorption domains for organic compounds: a review. Environmental Science and Technology 43, 1680–1688.
Chefetz, B.D., Hatcher, P.G., Guthrie, E.A., 2000. Pyrene sorption by natural organic matter. Environmental Science and Technology 34, 2925–2930.
Chen, B., Xing, B., 2005. Sorption and conformational characteristics of reconstituted plant cuticular waxes on montmorillonite. Environmental Science and Technology 39, 8315–8323.
Chen, Y., Sheng, G., Bi, X., Feng, Y., Mai, B., Fu, J., 2005. Emission factors for carbonaceous particles and polycyclic aromatic hydrocarbons from residential coal combustion in China. Environmental Science and Technology 39, 1861–1867.
Chiou, C.T., Shoup, T.D., 1985. Soil sorption of organic vapors and effects of humidity on sorptive mechanism and capacity. Environmental Science and Technology 19, 1196–1200.
Chiou, C.T., Kile, D.E., Malcolm, R.L., 1988. Sorption of vapors of some organic liquids on soil humic acid and its relation to partitioning of organic compounds in soil organic matter. Environmental Science and Technology 22, 298–303.
Corley, T.L., Farrell, J., Hong, B., Conklin, M.H., 1996. VOC accumulation and pore filling in unsaturated porous media. Environmental Science and Technology 30, 2884–2891.
Cornelissen, G., Gustafsson, O., Bucheli, T.D., Jonker, M.T.O., Koelmans, A.A., van Noort, P.C.M., 2005. Extensive sorption of organic compounds to black carbon, coal, and kerogen in sediments and soils: mechanisms and consequences for distribution, bioaccumulation, and biodegradation. Environmental Science and Technology 39, 6881–6895.
Crittenden, J.C., Sanongraj, S., Bulloch, J.L., Hand, D.W., Rogers, T.N., Speth, T.F., Ulmer, M., 1999. Correlation of aqueous-phase adsorption isotherms. Environmental Science and Technology 33, 2926–2933.
de Jonge, H., Mittelmeijer-Hazeleger, M.C., 1996. Adsorption of CO_2 and N_2 on soil organic matter: nature of porosity, surface area, and diffusion mechanisms. Environmental Science and Technology 30, 408–413.
Dubinin, M.M., 1960. The potential theory of adsorption of gases and vapors for adsorbents with energetically nonuniform surfaces. Chemical Reviews 60, 235–241.
Durand, B., 1980. Sedimentary organic matter and kerogen. Definition and quantitative importance of kerogen. In: Durand, B. (Ed.), Kerogen: Insoluble Organic Matter From Sedimentary Rocks. Editions Technip, Paris, pp. 13–35.
Farrell, J., Reihard, M., 1994a. Desorption of halogenated organics from model solids, sediments, and soil under unsaturated conditions. 1. Isotherms. Environmental Science and Technology 28, 53–62.
Farrell, J., Reihard, M., 1994b. Desorption of halogenated organics from model solids, sediments, and soil under unsaturated conditions. 2. Kinetics. Environmental Science and Technology 28, 63–72.
Filimonova, S.V., Knicker, H., Häusler, W., Kögel-Knabner, I., 2004. ^{129}Xe NMR spectroscopy of adsorbed xenon as an approach for the characterisation of soil meso- and microporosity. Geoderma 122, 25–42.
Gan, H., Nandi, S.P., Walker Jr., P.L., 1972. Nature of the porosity in American coals. Fuel 51, 272–277.
Grathwohl, P., 1990. Influence of organic matter from soils and sediments from various origins on the sorption of some chlorinated aliphatic hydrocarbons: implications on Koc correlations. Environmental Science and Technology 24, 1687–1693.
Gregg, S.J., Sing, K.S.W., 1982. Adsorption, Surface Area and Porosity, 2nd ed. Academic Press, London.
Harris, L.A., Yust, C.S., 1976. Transmission electron microscope observations of porosity in coal. Fuel 55, 233–236.
Huang, W., Weber, W.J., 1997. A distributed reactivity model for sorption by soils and sediments. 10. Relationships between desorption, hysteresis, and the chemical characteristics of organic domains. Environmental Science and Technology 31, 2562–2569.
Kleineidam, S., Schuth, C., Grathwohl, P., 2002. Solubility-normalized combined adsorption-partitioning sorption isotherms for organic pollutants. Environmental Science and Technology 36, 4689–4697.
Kögel-Knabner, I., 1997. ^{13}C and ^{15}N NMR spectroscopy as a tool in soil organic matter studies. Geoderma 80, 243–270.
Kwon, S., Pignatello, J.J., 2005. Effect of natural organic substances on the surface and adsorptive properties of environmental black carbon (char): pseudo pore blockage by model lipid components and its implications for N2-probed surface properties of natural sorbents. Environmental Science and Technology 39, 7932–7939.
Larsen, J.W., Hall, P., Wernett, P.C., 1995. Pore structure of the Argonne premium coals. Energy & Fuels 9, 324–330.
Li, J., Werth, C.J., 2001. Evaluating competitive sorption mechanisms of volatile organic compounds in soils and sediments using polymers and zeolites. Environmental Science and Technology 35, 568–574.
Lin, T.-F., Van Loy, M.D., Nazaroff, W.W., 1996. Gas-phase transport and sorption of benzene in soil. Environmental Science and Technology 30, 2178–2186.
Mao, J.-D., Hundal, L.S., Thompson, M.L., Schmidt-Rohr, K., 2002. Correlation of poly(methylene)-rich aliphatic domains in humic substances with sorption of a nonpolar organic contaminant, phenanthrene. Environmental Science and Technology 36, 929–936.
Pignatello, J.J., Xing, B., 1996. Mechanisms of slow sorption of organic chemicals to natural particles. Environmental Science and Technology 30, 1–11.
Plaza, C., Xing, B., Fernández, J.M., Senesi, N., Polo, A., 2009. Binding of polycyclic aromatic hydrocarbons by humic acids formed during composting. Environmental Pollution 157, 257–263.
Ran, Y., Huang, W.L., Rao, P.S.C., Liu, D.H., Sheng, G.Y., Fu, J.M., 2002. The role of condensed organic matter in the nonlinear sorption of hydrophobic organic contaminants by a peat and sediments. Journal of Environmental Quality 31, 1953–1962.
Ran, Y., Xing, B., Rao, P.S.C., Fu, J., 2004. Importance of adsorption (hole-filling) mechanism for hydrophobic organic contaminants on an aquifer kerogen isolate. Environmental Science and Technology 38, 4340–4348.
Ran, Y., Sun, K., Yang, Y., Xing, B., Zeng, E., 2007. Strong sorption of phenanthrene by condensed organic matter in soils and sediments. Environmental Science and Technology 41, 3952–3958.
Ran, Y., Yang, Y., Xing, B., Pignatello, J.J., Kwon, S., Su, W., Zhou, L., 2013. Evidence of micropore-filling for sorption of nonpolar organic contaminants by condensed organic matter. Journal of Environmental Quality 42, 806–814.
Ravikovitch, P.I., Bogan, B.W., Neimark, A.V., 2005. Nitrogen and carbon dioxide adsorption by soils. Environmental Science and Technology 39, 4990–4995.
Reucroft, P.J., Sethuraman, A.R., 1987. Effect of pressure on carbon dioxide induced coal swelling. Energy & Fuels 1, 72–75.
Salloum, M.J., Chefetz, B., Hatcher, P.G., 2002. Phenanthrene sorption by aliphatic-rich natural organic matter. Environmental Science and Technology 36, 1953–1958.
Senesi, N., 1992. Binding mechanisms of pesticides to soil humic substances. Science of the Total Environment 123–124, 63–76.
Vorres, K.S., 1990. The Argonne premium coal sample program. Energy & Fuels 4, 420–426.
Walker Jr., P.L., Kini, K.A., 1965. Measurement of the ultrafine surface area of coals. Fuel 453–459.
Weber, W.J., McGinley, P.M., Katz, L.E., 1992. A distributed reactivity model for sorption by soils and sediments. 1. Conceptual basis and equilibrium assessments. Environmental Science and Technology 26, 1955–1962.
Weber, W.J., Kim, S.H., Johnson, M.D., 2002. Distributed reactivity model for sorption by soils and sediments. 15. High-concentration co-contaminant effects on phenanthrene sorption and desorption. Environmental Science and Technology 36, 3625–3634.
Xing, B., Pignatello, J.J., 1997. Dual-mode sorption of low-polarity compounds in glassy poly(vinyl chloride) and soil organic matter. Environmental Science and Technology 31, 792–799.
Zhu, D., Hyun, S., Pignatello, J.J., Lee, L.S., 2004. Evidence for π − π electron donor − acceptor interactions between π-donor aromatic compounds and π-acceptor sites in soil organic matter through pH effects on sorption. Environmental Science and Technology 38, 4361–4368.